Activities of α-COOH vs γ-COOH in *N*-Phosphoryl Amino Acids: A Theoretical Study

Zhong-Zhou Chen,[†] Yan-Mei Li,*[,†] Jing Ma,[‡] Bo Tan,[†] Satoshi Inagaki,[§] and Yu-Fen Zhao[†]

Key Laboratory for Bioorganic Phosphorus Chemistry of Education Ministry, Department of Chemistry, School of Life Sciences and Engineering, Tsinghua University, Beijing 100084, P. R. China, Department of Chemistry, Nanjing University, Nanjing 210093, P. R. China, and Department of Chemistry, Faculty of Engineering, Gifu University, Yanagido, Gifu 501-1193, Japan

Received: May 2, 2002; In Final Form: September 23, 2002

The biomimic reactions of *N*-phosphoryl amino acids are very important in the study of many biochemical processes, such as origin of proteins and phosphorylation of amino acid residues in the proteins. The differences in reactivities between α-COOH and γ-COOH in phosphoryl amino acids were studied by ab initio and density functional methods. The pentacoordinate phosphoric intermediates **2** containing five-membered rings were predicted to be more stable than **3** with seven-membered rings. For intermediates **3**, the isomers with apical-equatorial ring spanning arrangement were predicted to be more stable than those with diequatorial ring spanning arrangement. At the B3LYP/6-31G** level, intermediates **2** were 66.56 kJ/mol lower in energy than **3**. It was shown that the transition states **4** and **5** involving an α-COOH or γ-COOH group had energy barriers of $\Delta E = 57.59$ kJ mol^{-1} and 120.93 kJ mol^{-1}, respectively. The theoretical calculations suggested that the α-COOH group could be differentiated from the γ-COOH intramolecularly in amino acids by *N*-phosphorylation. These might be helpful to understand why only α-COOH, not γ-COOH, was involved in the biomimic reactions.

Introduction

It is well-known that α-peptides take secondary conformations. Recently, it has been found that γ-peptides also adopt secondary conformations, such as helical conformation,[1a,1b] parallel sheet,[1c] and reverse turn.[1d] γ-Peptides, such as glutathione and oligo(γ-glutamyl), also have biological activities.[2] Nonenzymatic deamidation of glutamine residue in biologically important proteins may be an important prerequisite for the stability of proteins in vivo, such as in the lens of the human eye.[3] γ-Glutamyl peptide was found in the nonenzymatic deamidation of glutaminyl peptide under physiological conditions.[4] In addition, the content of γ-peptide was higher than that of α-peptide. Nevertheless, nature chose α-amino acids to be the backbone of the proteins. This raises the question of why nature chose α-amino acids, rather than γ-amino acids, as the protein skeleton.

Many biological processes are regulated by the phosphorylation and dephosphorylation of amino acid residues in proteins.[5] Formation of high-coordinate phosphoric intermediates is usually described as a key step in most enzyme catalytic mechanisms.[6] Study of cyclic phosphoric compounds had proven their usefulness as models for intermediates in enzymatic reactions of cyclic adenosine monophosphate and for nonenzymatic reactions of tetracoordinated phosphates.[7]

It has been shown in our laboratory that *N*-phosphoryl amino acids and peptides are chemically active species that characterize biomimic reactivities,[8] such as ester exchange on phosphorus, peptide formation, and esterification, which might be related to the prebiotic synthesis of proteins and nucleotides.[9] Meanwhile, since *N*-phosphoryl amino acids have a tetrahedral structure similar to the inhibitors of metallopeptidases,[10] they are of pharmaceutical interest. An intramolecular pentacoordinate carboxylic−phosphoric mixed anhydride has been proposed as the common intermediate for the biomimic reactions of phosphoryl amino acids and peptides.[11] The silylated intramolecular mixed carboxylic−phosphoric anhydrides have been synthesized and identified.[12,13] However, the high and multifunctional reactivities of *N*-phosphoryl amino acids under mild conditions is difficult to explain. Theoretical study on the mechanism of the biomimic reactions can provide important information for the phosphorus participation in biochemistry.

In our previous paper, the activity difference between α-COOH and γ-COOH was studied by MNDO methods.[14] However, the semiempirical MNDO calculations did not clearly distinguish the activity difference between α-COOH and γ-COOH. Further calculations with more elaborate methods were needed. To avoid the effect of the conformations of different phosphoryl amino acids, phosphoryl glutamic acid, with both α-COOH and γ-COOH in one molecule, was selected. It is very useful to know which carboxylic group in glutamic acid is involved in biomimic reactions theoretically.

Modeling and Computational Details

N-Dimethylphosphoryl L-glutamic acid (DMP-Glu, **1**) was taken as the model reactant[15] and the possible mechanisms of forming pentacoordinate phosphoric intermediates were shown in Scheme 1. There are two possible mechanisms from reactant **1**; one is through pentacoordinate phosphoric intermediates **2** by the attack of α-COOH (path A), and the other is through **3** by γ-COOH (path B).

Transition states were found by Synchronous Transit-Guided Quasi-Newton (STQN) methods[16] at the HF/6-31G** and B3LYP[17]/6-31G** level, and confirmed by frequency calculations and intrinsic reaction coordinate (IRC) calculations. Natural

* Corresponding author.
[†] Tsinghua University.
[‡] Nanjing University.
[§] Gifu University.

10.1021/jp021110q CCC: $22.00
Published on Web 10/29/2002

SCHEME 1: Possible Reaction Mechanisms Involved in Forming Penta-coordinate Phosphoric Intermediates from *N*-Phosphoryl Glutamic Acid

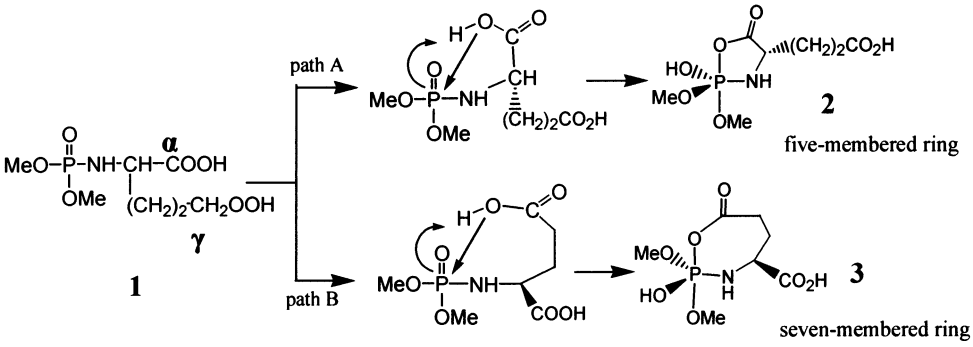

bond orbital (NBO) analysis[18] and frequency calculations were performed at the same level. Corrections of zero-point vibrational energies (ZPE) were made for all energies at the B3LYP/6-31G** level. Single-point calculations were performed at the B3LYP/6-311+G**//B3LYP/6-31G** level. The solvent effects were calculated by a polarized continuum (PCM) model[19] and Langevin Dipoles (LD) model[20] at the B3LYP/6-31G** level. The calculated free energies in solution were taken as the energies calculated in the gas phase (including ZPE) plus the solvent shift calculated at the B3LYP/6-31G** level.[21] The relative energies (RE) in this paper referred to the energies relative to DMP-Glu (**1**).

All quantum chemistry calculations were carried out with Gaussian 98 software[22] on a Power Challenge R12000 workstation. All molecular modeling was performed on an SGI workstation with the SYBYL6.7 software package (Tripos Inc., St. Louis, MO, 2000).

Results and Discussions

The crystal structure of *N*-diisopropylphosphoryl (DIPP) alanine was reported from our laboratory previously.[23] The model molecule DMP-Glu (**1**) was optimized at the B3LYP/6-31G** level, with geometry as shown in Figure 1. In **1**, the dihedral angles of O3−P1−N2−H4, O3−P1−O7−C8, and C6−O5−P1−O3 were calculated to be 29.1°, 57.3°, and 38.0°, respectively, being in agreement with the crystal geometry of DIPP−Ala with the corresponding dihedral angles of 4.3°, 56.6°, and 39.6°, respectively. Only the N−H bond in **1** partly departed from the N−P═O plane. So the geometry of **1** was rational.

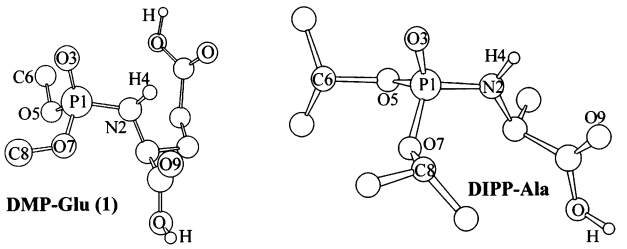

Figure 1. Structure DMP−Glu at the B3LYP/6-31G** level and the crystal structure of DIPP−Ala.

Then, to determine which group, α- or γ-carboxylic group in phosphoryl glutamic acid**,** might be involved in the formation of the pentacoordinate phosphoric intermediates easily, we performed the following theoretical studies.

Reactivity of the Two Anions of DMP-Glu. α- and γ-carboxylic anions can be obtained from **1**, and their optimized geometries at the HF/6-31G** level are shown in Figure 2. The α-CO_2^- anion was 18.80 kJ/mol more stable than the γ-CO_2^- anion. During optimization at the B3LYP/6-31G** level, the γ-CO_2^- anion was not stable and was converted to the α-CO_2^- anion. The dihedral angles of O3−P1−N2−H4 in α- and γ-carboxylic anions were found to be 176.7° and 75.8°, respectively, differing greatly from those in **1**. Figure 2 shows two intramolecular hydrogen bonds formed in the α-anion and γ-anion, respectively. The angle of N2−H4···O5 in the α-anion was 14° larger than that in the γ-anion. Meanwhile, the NBO absolute charges of O5 and H4 in the α-CO_2^- anion were 0.0853 and 0.0143 larger than those in γ-CO_2^- anion, respectively. So the intramolecular hydrogen bond N2−H4···O5 made the α-anion more stable. This makes the nucleophilic attack of an α-COOH group on the phosphorus atom more favored. As a result, the formation of the pentacoordinate phosphoric intermediates from an α-COOH group might be easier.

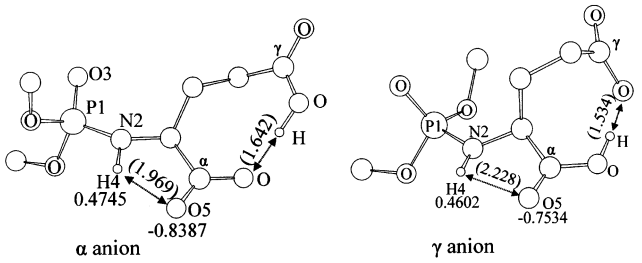

Figure 2. α-Anion and β-anion from DMP−Glu optimized at the HF /6-31G** level. The NBO atomic charges and the distances (in parentheses, Å) were shown in the figures.

Isomers of Intermediates 2 and 3. There may exist two types of pentacoordinate phosphoric intermediates **2** and **3**, containing a five-membered ring formed by an α-carboxylic group and a seven-membered ring by a γ-carboxylic group, respectively (Scheme 1). It is well-known that pentacoordinate phosphoric intermediates **2** and **3** prefer *tbp* (trigonal bipyramidal) configurations, in which the apical bonds are longer than the equatorial ones, for no bicyclic rings and an electronic imbalance of five different ligands.[24] There are six positional isomers with the ring in apical-equatorial spanning arrangement for **2** and **3**, respectively. These isomers can be divided into two classes: the first class were the isomers in which the P−N bond was in apical position, the second class were those in the equatorial position. The pentacoordinate phosphoric intermediates were calculated by the MNDO method[14] or at the B3LYP/6-31G** level (for DMP−Ala), it was found that the latter was more stable than the former, owing to the higher apicophilicity of the oxygen atom. Experimentally, it had been shown that the P−O bond of the anhydride P−O−CO moiety was an apical bond.[12b] Therefore, the positional isomers with the P−N bond in an apical position were not calculated in this paper.

TABLE 1: Relative Energies (RE, kJ/mol) of Penta-coordinate Phosphoric Intermediates at the HF/6-31G Level**[a]

compounds	RE	compounds	RE	compounds	RE
2a	69.55	**3a**	123.09	**3g**	164.39
2b	47.32	**3b**	117.20	**3h**	168.50
2c	47.09	**3c**	115.42	**3i**	154.42

[a] **2** and **3** stand for compounds containing five or seven-member ring, respectively. Hydroxyl group is on the ring plane for **a**, **g**; at the different side of the rest carboxylic group for **b, h**; at the same side for **c, i**. The nomenclature is the same as ref 14.

For intermediates **2**, there were three isomers (**2a**−**2c**) calculated in this paper, while six isomers (**3a**−**3c, 3g**−**3i**)[14] for intermediates **3**, because the arrangement of the seven-membered ring might be apical-equatorial spanning or diequatorial spanning.[25] To find the most stable conformers in each kind of intermediates**,** nine isomers were optimized at the HF/6-31G** level with their relative energies listed in Table 1. The isomer **2c** and **3c** were most stable among intermediates **2** and **3**, respectively. Meanwhile, isomer **3i** was most stable among intermediates **3** with the seven-membered ring in a diequatorial spanning arrangement. For each kind of isomers, the most stable structures were those in which the hydroxyl group and the residual carboxylic group were at the same side of the ring due to low bulkiness of the hydroxyl group. Hence, the steric hindrance of the phosphorus atom was reduced in the most stable conformers.

Comparison of the Intermediates 2c, 3c, and 3i. At the B3LYP/6-31G** level, the optimized geometries of **2c**, **3c,** and **3i** are depicted in Figure 3. It can be seen that geometries **2** and **3** were twisted trigonal bipyramid, in agreement with predictions.[26] The atoms in the five-membered ring were almost coplanar. In apical-equatorial spanning arrangement **3c**, the seven-membered ring was in a form like a boat. For diequatorial spanning arrangement **3i**, the seven-membered ring was in a form like a chair. These two types of arrangements were similar to those from DMP−Asp.[15] The main geometric parameters in **2c** and **3c** were quite different at the B3LYP/6-31G** level (Figure 3). The bond length of P1−O3 and the distance between the P1 and O6 atom in **2c** were 0.067 and 0.989 Å longer than those in **3c**, making **2c** less crowded. The absolute NBO charges of P1, C5, and O3 in **2c** were 0.0271, 0.0129, and 0.0436 lower than those in **3c**, respectively. These implied that **3c** had higher activity. In addition, a hydrogen bond N2−H4···O6 was formed in **2c**. It was also found that **2c** containing hydrogen bond N2−H4···O6 was about 13 kJ/mol less in energy than that with hydrogen bond N2−H4···O7 at the B3LYP/6-31G** level, due to the stronger electron-donating ability of the carbonyl group. Therefore, the side chain carbonyl group makes intermediates **2c** more stable (Table 2). The intermediates **2** containing five-membered rings were more stable than **3** with seven-membered rings.

Comparing isomer **3c** with **3i**, the arrangements of the seven-membered ring differed greatly. The P−O3 bond in the anhydride P−O−CO moiety was reduced more than that in P−O−R when changed from apical bond to equatorial bond, so **3i** was more crowded than **3c**. The angle of N2−P1−O3 in **3i** was 112.6°, which was lower than the standard angle of *tbp* configuration. These implied that the strain in structure **3i** was higher than that in **3c**. The NBO charges of P1 and C5 in **3i** were 0.0038 and 0.0129 larger than that in **3c**, making **3i** more active. Therefore, the energy difference between the two arrangements was so large (40 kJ/mol) that intermediates **3** should exist in apical-equatorial spanning. This was supported by experiments and theoretical calculations.[7,12b,25]

Strain Energies of the Intermediates 2c, 3c, and 3i. To understand the relative stabilities, the strain energies were calculated from the homodesmotic reactions[27] at the B3LYP/6-31G** level. The calculated strain energies are listed in Table 3. The strain energy of the five-membered ring in **2c** was found to be the lowest and negative, similar to the results of the pentagon stability for compounds containing phosphorus ring.[28] The low strain energy may be attributed to the high *p*-character of the hybrid orbital on the P atom for the P1−O3 bond or to the resulting stabilization by the delocalization of σ electrons to and from the geminal P1−N2 bond due to the $\sigma \rightarrow \sigma^*$ orbital interaction[29] in **2c**. The geminal delocalization relaxes the ring strain, leading to the relative stablity of the five-membered ring.

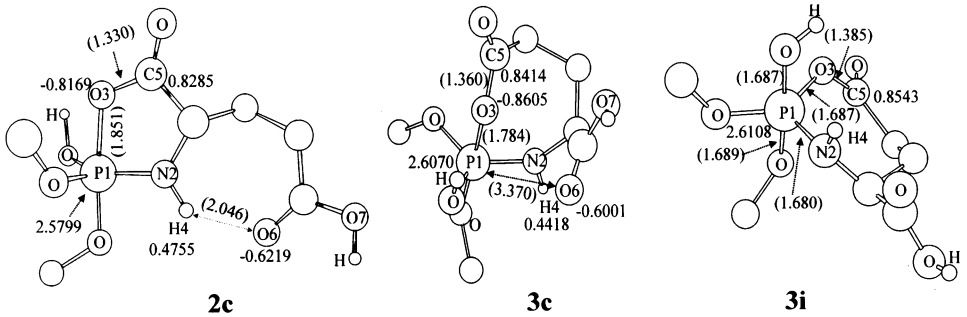

Figure 3. Optimized structures of **2c**, **3c,** and **3i** at the B3LYP/6-31G** level. The NBO atomic charges and the distances (in parentheses, Å) were shown in the figures.

TABLE 2: Relative Energies (RE) of Key Intermediates and Transition States

RE (kJ/mol)	HF/6-31G**	B3LYP/6-31G**	B3LYP/6-311+G** // B3LYP/6-31G**[a]	energies in *n*-BuOH[b]	energies in water[b]	energies in water[c]
2c	47.09	19.64	31.62	21.18	13.52	34.70
4	104.90	57.59	78.76	67.24	60.52	51.73
3c	115.42	86.20	99.02	86.15	77.68	97.50
5	158.84	120.93	136.38	119.89	111.29	104.61
3i	154.42	120.70	131.92	121.32	113.22	135.34
ΔE(3c−2c)	68.33	66.56	67.40	64.97	64.16	62.8

[a] Single-point B3LYP/6-311+G**//B3LYP/6-31G** energies do not include solvent energies. [b] Energies were calculated by PCM model at the B3LYP/6-31G** level. [c] Energies were calculated by Langevin dipoles model at the B3LYP/6-31G** level. ZPE had been considered for all the energies at the B3LYP/6-31G** level.

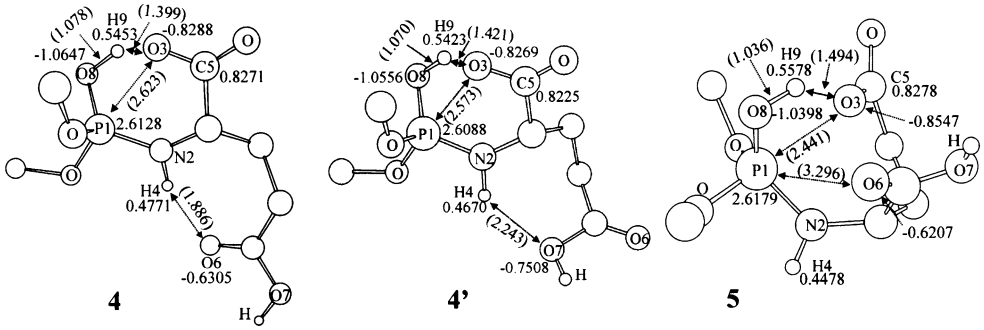

Figure 4. Optimized structures of **4**, **4′**, and **5** at the B3LYP/6-31G** level. The NBO atomic charges and the distances (in parentheses, Å) were shown in the figures.

TABLE 3: Strain Energies and Interbond Energies (kJ/mol) in Ring

molecule	strain energies	σ_1[a] bond hybrid P1	σ_1[a] bond hybrid O3	interbond energies[b] $\sigma_1 \cdot \sigma_2^*$	$\sigma_2 \cdot \sigma_1^*$	$\sigma_1^* \cdot \sigma_2^*$
2c	−52.49	$sp^{3.58}d^{2.78}$	$sp^{3.34}$	164.36	90.37	367.69
3c	31.06	$sp^{3.40}d^{2.35}$	$sp^{2.88}$	128.53	77.95	183.47
3i	59.67	$sp^{3.44}d^{0.86}$	$sp^{2.62}$	−	−	−

[a] σ_1 and σ_2 were referred as P1−N2, P1−O3 bond, respectively. [b] − means less than 2.0 kJ/mol.

Although the B3LYP/6-31G** relative energies were lower than the single-point B3LYP/6-311+G**//B3LYP/6-31G** energies in Table 2, the energy differences were close to each other. It implied that the energies at the B3LYP/6-31G** level were good enough. Comparing HF results and B3LYP results with 6-31G** basis sets, it was found that the relative energies from the HF calculations were higher than those from the B3LYP calculations, and the bond lengths at the HF/6-31G** level were about 0.02∼0.04 Å lower than those at the B3LYP/6-31G** level (Table 2). Since the effect of electron correction was omitted within the Hartree−Fock theory, HF/6-31G** levels were not good enough to produce accurate results.

Geometries of the Transition States. Isomers **2c** and **3c** were the most stable isomers of the corresponding intermediates and were selected for searching for the corresponding transition states. The transition states **4** and **5** were fully optimized by the STQN[16] method at the HF/6-31G** and B3LYP/6-31G** levels. Their geometries at the B3LYP/6-31G** level are shown in Figure 4. In their frequency calculations, **4** and **5** each had only one imaginary frequency at 337.92i and 168.89i cm^{-1}, respectively. The vibrational modes corresponding to the imaginary vibrational frequencies of **4** and **5** and the IRC calculations showed that the optimized structures were true transition states with one imaginary frequency corresponding to the proton H9 transfer and the bond P1−O3 formation. Therefore, the proton transfer and the bond formation of P1−O3 were cooperative in the formation of the intermediates.

According to Figure 4, transition states **4** or **5** both contained a hydrogen-bond bridge structure O8−H9−O3. From the NBO bond analysis, the O3 atom interacted with the unoccupied orbital of the phosphorus atom and the antibonds of H9−O8. Compared with reactant **1**, H9−O8 and P1−O3 bonds were partially formed in transition states **4** and **5**. The shorter distance between O3 and P1, and the participation of the O6 atom made the phosphorus atom in **5** more crowded than in **4**. In addition, the NBO absolute atomic charges of P1, O3 and H9 in **5** were 0.0051, 0.0259, and 0.0125 larger than those in **4**, respectively. These made transition state **5** more active. As a result, **4** was more stable than **5**. A hydrogen bond N2−H4···O6 was formed in **4.** For another transition state **4′** (Figure 4) with a hydrogen bond N2−H4···O7, the energy was 21.70 kJ/mol higher than that of **4**. Comparing transition states **4** and **4′**, the structures differed greatly. The strong electron-donating ability of the carbonyl oxygen atom O6 made the hydrogen bond in **4** stronger than **4′**, and the structure **4** less crowded. In addition, the transition state from **2b** was also obtained because the energy difference between **2b** and **2c** was small, with the energy 8.09 kJ/mol higher than **4**. It also had a hydrogen bond N2−H4···O6. Therefore, the side chain greatly lowered the energies of transition states. It could explain why *N*-phosphoryl amino acids containing a polar side chain showed high activities experimentally.[14]

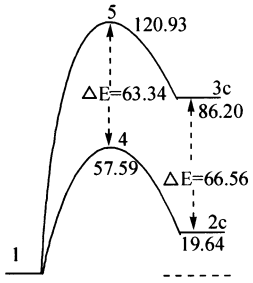

Figure 5. Energies (kJ/mol) profile for reactant, intermediates, and transition states at the B3LYP/6-31G** level.

Solvation Effect. The energy profiles of the cooperative mechanisms are shown schematically in Figure 5. The energy barrier of forming **4** was 63.34 kJ mol^{-1} lower than that of **5**. The peptide formation of *N*-phosphoryl amino acids was carried out in organic solvent experimentally.[14] The solvent effects were calculated by using the PCM model[19] in *n*-butanol ($\epsilon = 15.0$) and water (Table 2). For the reactions in path A and path B**,** the solvent effect was different. It increased the energy barrier in forming **2c**, but decreased the energy barrier of forming **3c**. For the reaction in aqueous solution, the Langevin dipoles (LD) model had many advantages. In the LD model, the solvent was approximated by polarizable dipoles and the charges were obtained from the PCM continuum model. It[30] takes into account the polarization of the solute molecules by the solvent and the corresponding energy contributions. As shown in Table 2, the solvation energies were reasonable. The dipole moments of **4** and **5** were larger than **1**, and their relative energies in aqueous solution were lower than in gas phase.

Summary and Conclusion

Theoretical calculations are useful to solve the biochemical questions, such as the activity difference between α-COOH and γ-COOH. Compared to the PCM model, the Langevin dipoles model had many advantages for the reaction in aqueous reaction. The calculations predicted that the formation of pentacoordinate intermediates was cooperative and the side chain promoted the

formation by forming a hydrogen bond. They showed that α-COOH activated the phosphoryl group intramolecularly by forming a phosphoric−carboxylic mixed anhydride intermediate containing a five-membered ring, while γ-COOH group formed the seven-membered analogue unfavorably. These results implied that the formation of pentacoordinate phosphoric intermediates followed path A and that the reaction could occur in mild conditions, as was indeed observed in the experiments. This is consistent with the fact that only α-COOH unprotected phosphoryl amino acids could undergo the biomimic reactions.[31] These results might be helpful to understand the selectivity in the biomimic reactions of phosphoryl amino acids and to answer the question as to why nature chose α-amino acids in the origin of proteins.

Acknowledgment. The authors thank Dr. Jan Florian for kindly help. We are also grateful for the financial support from the Chinese National Natural Science Foundation (No. 29802006), the Teaching and Research Award Program for Outstanding Young Teachers in Higher Education Institutions of MOE, P.R.C. and Tsinghua University.

Supporting Information Available: Cartesian matrixes of two anions optimized at the HF/6-31G** level; Geometries **1**, **2c**, **3c**, **3i**, transition states **4**, **4′**, **4″**, and **5** optimized at the B3LYP/6-31G** level; The optimized structures of **2a**, **2b**, **2c**, **3a**, **3b**, **3c**, **3g**, **3h**, **3i** at the HF/6-31G** level; The ring conformations of **3c** and **3i**; The vibration mode corresponding to the imaginary frequency of **4** and **5**; Homodesmotic reactions for calculating the strain energies of **2c**, **3c**, and **3i**. The optimized structures and the relative energies of **4′** (containing hydrogen bond in N2−H4···O7**)** and **4″** (the transition states corresponding to **2b**); The solvation results from the Langevin dipoles model at the B3LYP/6-31G** level. This material is available free of charge via the Internet at http://pubs.acs.org.

References and Notes

(1) (a) Hintermann, T.; Gademann, K.; Jaun, B.; Seebach, D. *Helv. Chim. Acta* **1998**, *81*, 983. (b) Hanessian, S.; Luo, X. H.; Schaum, R.; Michnick, S. *J. Am. Chem. Soc.* **1998**, *120*, 8569. (c) Woll, M. G.; Lai, J. R.; Guzei, I. A.; Taylor, S. J. C.; Smith, M. E. B.; Gellman, S. H. *J. Am. Chem. Soc.* **2001**, *123*, 11077. (d) Hanessian, S.; Luo, X. H.; Schaum, R. *Tetrahedron Lett*. **1999**, *40*, 4925.

(2) (a) Hammond, C. L.; Lee, T, K.; Ballatori, N. *J. Hepatol*. **2001**, *34*, 946. (b) Bisset, G. M. F.; Pawelczak, K.; Jackman, A. L.; Calvert, A. H.; Hughes, L. R. *J. Med. Chem.* **1992**, *35*, 859.

(3) (a) Takemoto, L.; Boyle, D. *Biochemistry* **1998**, *37*, 13681. (b) Robinson, A. B.; Robinson, L. R. *Proc. Natl. Acad. Sci. U.S.A.* **1991**, *88*, 8880.

(4) (a) Schucker, S. C.; Scriba, G. K. E. *J. Chromatogr. A* **2000**, *888*, 275. (b) Capasso, S.; Mazzarella, L.; Sica, F.; Zargari, A. *J. Chem. Soc., Chem. Commun.* **1991**, 1667.

(5) Stock, J. B.; Ninfa, A. J.; Stock, A. M. *Microbiol. Rev.* **1989,** *53*, 450.

(6) (a) Senior, A. E.; Nadanaciva, S.; Weber, J. *J. Exp. Biol*. **2000**, *203*, 35. (b) Bernstein, B. E.; Michels, P. A. M.; Hol, W. G. J. *Nature* **1997**, *385*, 275. (c) Skordalakes, E.; Dodson, G. G.; Green, D. S.; Goodwin, C. A.; Scully, M. F.; Hudson, H. R.; Kakkar, V. V.; Deadman, J. J. *J. Mol. Biol.* **2001**, *311*, 549.

(7) Holmes, R. R.; Day, R. O.; Deiters, J. A.; Kumara-Swamy, K. C.; Homles, J. M.; Hans, J.; Burton, S. D.; Prakasha, T. K. In *Phosphorus Chemistry: Developments in American Science*; Walsh, E. N., Griffith, E. J., Parry, R. W., Quin, L. D. Eds.; ACS Symposium Series 486; American Chemical Society: Washington, DC, 1992; pp 18−40.

(8) (a) Xue, C. B.; Yin, Y. W.; Zhao, Y. F. *Tetrahedron Lett.* **1988**, *29*, 1145. (b) Ma, X. B.; Zhao, Y. F. *J. Org. Chem.* **1989**, *54*, 4005. (c) Zhao, Y. F.; Ju, Y.; Li, Y. M.; Wang, Q.; Yin, Y. W.; Tan, B. *Int. J. Pept. Protein Res*. **1995**, *45*, 514.

(9) (a) Zhao, Y. F.; Cao, P. S. *J. Biol. Phys*. **1994**, *20*, 283. (b) Ju, Y.; Zhao, Y. F.; Sha, Y. W.; Tan, B. *Phosphorus, Sulfur Silicon Relat. Elem.* **1995**, *101*, 117. (c) Zhao, Y. F.; Li, Y. M.; Yin, Y. W.; Li, Y. C. *Sci. China, Ser. B−Chem.* **1993**, *36*, 561.

(10) Rowsell, S.; Pauptit, R. A.; Tucker, A. D.; Melton, R. G.; Blow, D. M.; Brick, P. *Structure* **1997**, *5*, 337.

(11) (a) Zhong, R. G.; Zhao, Y. F.; Dai, Q. H. *Chin. Sci. Bull.* **1998**, *43*, 917. (b) Ramirez, F.; Marecek, J. F.; Okazaki, H. *J. Am. Chem. Soc.* **1976**, *98*, 5310.

(12) (a) Wang, Q.; Zhao, Y. F.; An, F. L.; Mao, Y. Q.; Wang, Q. Z. *Sci. China Ser. B−Chem.* **1995**, *25*, 683. (b) Fu, H.; Tu, G. Z.; Li, Z. L.; Zhao, Y. F.; Zhang, R. Q. *J. Chem. Soc., Perkin Trans. 1* **1997**, 2021.

(13) Fu, H.; Li, Z. Z.; Zhao, Y. F.; Tu, G. Z. *J. Am. Chem. Soc.* **1999**, *121*, 291.

(14) Chen, Z. Z.; Tan, B.; Li, Y. M.; Chen, Y.; Cheng, C. M.; Zhao, Y. F. *J. Mol. Struct.−Theochem.* **2001**, *574*, 163.

(15) Chen, Z. Z.; Tan, B.; Li, Y. M.; Zhao, Y. F. *Chin. Chem. Lett.* **2001**, *12*, 1093.

(16) Peng, C. Y.; Ayala, P. Y.; Schlegel, H. B.; Frisch, M. J. *J. Comput. Chem.* **1996**, *17*, 49.

(17) (a) Becke, A. D. *J. Chem. Phys.* **1993**, *93*, 5648. (b) Wu, Y. D.; Lai, D. K. W. *J. Am. Chem. Soc.* **1995**, *117*, 11327.

(18) Glendening, E. D.; Reed, A. E.; Carpenter, J. E.; Weinhold, F. *NBO Version 3.1*.

(19) (a) Miertus, S.; Scrocco, E.; Tomasi, J. *Chem. Phys.* **1981**, *55*, 117. (b) Miertus, S.; Tomasi, J. *Chem. Phys.* **1982**, *65*, 239. (c) Tomasi, J.; Persico, M. *Chem. Rev.* **1994**, *94*, 2027.

(20) Florian, J.; Warshel, A. *ChemSol, Version 2.0*; University of Southern California: Los Angeles, 1999.

(21) Zhan, C. G.; Zheng, F. *J. Am. Chem. Soc.* **2001**, *123*, 2835.

(22) Frisch, M. J.; Trucks, G. W.; Schlegel, H. B.; Scuseria, G. E.; Robb, M. A.; Cheeseman, J. R.; Zakrzewski, V. G.; Montgomery, J. A.; Stratmann, R. E.; Burant, J. C.; Dapprich, S.; Millam, J. M.; Daniels, A. D.; Kudin, K. N.; Strain, M. C.; Farkas, O.; Tomasi, J.; Barone, V.; Cossi, M.; Cammi, R.; Mennucci, B.; Pomelli, C.; Adamo, C.; Clifford, S.; Ochterski, J.; Petersson, G. A.; Ayala, P. Y.; Cui, Q.; Morokuma, K.; Malick, D. K.; Rabuck, A. D.; Raghavachari, K.; Foresman, J. B.; Cioslowski, J.; Ortiz, J. V.; Baboul, A. G.; Stefanov, B. B.; Liu, G.; Liashenko, A.; Piskorz, P.; Komaromi, I.; Gomperts, R.; Martin, R. L.; Fox, D. J.; Keith, T.; Al-Laham, M. A.; Peng, C. Y.; Nanayakkara, A.; Challacombe, M.; Gill, P. M. W.; Johnson, B.; Chen, W.; Wong, M. W.; Andres, J. L.; Gonzalez, C.; Head-Gordon, M.; Replogle, E. S.; Pople, J. A. *Gaussian 98* (Revision A.9); Gaussian, Inc.: Pittsburgh, PA, 1998.

(23) Xue, C. B.; Yin, Y. W.; Liu, Y. M.; Zhu, N. J.; Zhao, Y. F. *Phosphorus, Sulfur Silicon Relat. Elem.* **1989**, *42*, 149.

(24) Emsley, J.; Hall, D. *The Chemistry of Phosphorus: Environmental, Organic, Inorganic, Biochemical and Spectroscopic Aspects*; Harper & Row: London, 1976; pp 29−76.

(25) Corbridge, D. E. C. *Phosphorus: An Outline of Its Chemistry, Biochemistry and Technology*, 5th ed; Elsevier: New York, 1995; pp 1047−1126.

(26) (a) Holmes, R. R. *J. Am. Chem. Soc.* **1975**, *97*, 5379. (b) Holmes, R. R. *Phosphorus, Sulfur Silicon Relat. Elem.* **1995**, *98*, 89.

(27) (a) George, P.; Trachtman, M.; Bock, C. W.; Brett, A. M. *Tetrahedron* **1976**, *32*, 317. (b) The strain energy of **2c** was estimated from the enthalpy change of the homodesmotic reaction as shown below.

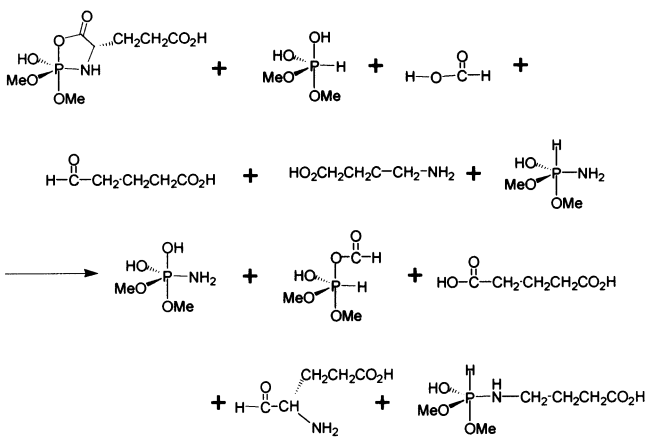

The strain energies of **3c** and **3i** were similar to **2c**.

(28) (a) Ma, J.; Hozaki, A.; Inagaki, S. *Inorg. Chem.* **2002**, *41*, 1876. (b) Schiffer, H.; Ahlrichs, R.; Haser, M. *Theor. Chim. Acta* **1989**, *75*, 1. (c) Gimarc, B. M.; Zhao, M. *Coordin. Chem. Rev.* **1997**, *158*, 385. (d) Ma, J.; Hozaki, A.; Inagaki, S. *Phosphorus, Sulfur Silicon Relat. Elem.* **2002**, *177*, 1705.

(29) (a) Inagaki, S.; Ishitani, Y.; Kakefu, T. *J. Am. Chem. Soc.* **1994**, *116*, 5954. (b) Inagaki, S.; Yoshikawa, K.; Hayano, Y. *J. Am. Chem. Soc.* **1993**, *115*, 3706. (c) Inagaki, S.; Goto, N.; Yoshikawa, K. *J. Am. Chem. Soc.* **1991**, *113*, 7144.

(30) (a) Florian, J.; Warshel, A. *J. Phys. Chem. B* **1999**, *103*, 10282. (b) Florian, J.; Warshel, A. *J. Phys. Chem. B* **1997**, *101*, 5583.

(31) Li, Y. M.; Zhang, D. Q.; Zhang, H. W.; Ji, G. J.; Zhao, Y. F. *Bioorg. Chem.* **1992**, *20*, 285.